Micro-ribonucleic acids (miRNAs) and a proteomic profile in lung adenocarcinoma cases with brain metastasis

Lingling Zhang[1#], Jianfeng Liang[2#], Zhiyi Han[3], Lihua Wang[4], Jun Liang[1], Shucai Zhang[5]

[1]Department of Oncology, Peking University International Hospital, Beijing, China; [2]Department of Neurosurgery, Peking University International Hospital, Beijing, China; [3]Department of Thoracic Surgery, Peking University International Hospital, Beijing, China; [4]Department of Pathology, Peking University International Hospital, Beijing, China; [5]Department of Medical Oncology, Beijing Chest Hospital, Capital Medical University, Beijing Tuberculosis and Thoracic Tumor Research Institute, Beijing, China

Contributions: (I) Conception and design: L Zhang, Jun Liang, S Zhang; (II) Administrative support: Jun Liang; (III) Provision of study materials or patients: L Wang; (IV) Collection and assembly of data: Z Han; (V) Data analysis and interpretation: L Zhang, Jianfeng Liang; (VI) Manuscript writing: All authors; (VII) Final approval of manuscript: All authors.

[#]These authors contributed equally to this work.

Correspondence to: Jun Liang, PhD. Department of Oncology, Peking University International Hospital, Beijing 102206, China. Email: junliang@pkuih.edu.cn; Shucai Zhang, PhD. Department of Medical Oncology, Beijing Chest Hospital, Capital Medical University, Beijing Tuberculosis and Thoracic Tumor Research Institute, Beijing 101149, China. Email: sczhang6304@163.com.

Background: Brain metastasis (BM) is the main cause of death of individuals with lung adenocarcinoma (LAC). Biomarkers with high sensitivity and specificity for the early detection and treatment of BM of LAC urgently need to be identified. In this study, we analyzed the pathogenesis of LAC-induced BM by detecting micro-ribonucleic acid (miRNA) and proteome expression differences between primary LAC lesion and BM tissue specimens to identify biomarkers of LAC-associated BM and develop potential therapeutic targets.

Methods: The miRNA and protein profiles of non-metastatic primary LAC and BM cases were examined to further explore the mechanism of BM. The roles and interactions of differential miRNAs and proteins were subject to Gene Ontology (GO) and Kyoto Encyclopedia of Genes and Genomes (KEGG) analyses. The interactions of differential miRNAs and proteins were analyzed by R software and depicted using Cytoscape.

Results: Compared to the LAC tissue specimens, 16 and 4 miRNAs showed increased and reduced levels, respectively, in the BM tissue specimens, and 53 proteins were upregulated, and 35 proteins were downregulated. The enrichment pathway analysis showed the nuclear factor kappa B (NF-κB) signaling and the primary immunodeficiency pathways played important roles in the pathogenetic mechanisms of BM in LAC.

Conclusions: This study extended understandings of the regulatory network of miRNAs and proteins and provided novel insights into the pathogenic mechanisms of BM in LAC at the miRNA and protein levels.

Keywords: Brain metastasis (BM); lung adenocarcinoma (LAC); miRNA; proteomics

Submitted Oct 28, 2022. Accepted for publication Dec 16, 2022.
doi: 10.21037/atm-22-5703
View this article at: https://dx.doi.org/10.21037/atm-22-5703

Introduction

Lung cancer is frequently associated with brain metastasis (BM), with about 40% of patients developing BM during the disease course (1). Non-small cell lung cancer (NSCLC) patients with BM have a very poor prognosis, and BM is the main cause of death in NSCLC (2). Without treatment, the post-BM survival time of such patients is only 1–2 months (2). The therapeutic efficacy of treatments

© Annals of Translational Medicine. All rights reserved.

remains unsatisfactory even though treatment options for BM currently include surgery, radiotherapy, chemotherapy, and immunotherapy. Thus, the biological and molecular mechanisms underlying BM in NSCLC urgently need to be studied to identify novel treatment targets.

Micro-ribonucleic acids (miRNAs) are considered an important component of the uncoded genome, and play major roles via a complex regulatory process in virtually all essential cellular events in various species (3). Previous studies have shown that miRNA expression profiles are associated with tumorigenesis, tumor progression, and treatment response; thus, such profiles could be used in diagnosis and prognosis prediction (4). Several miRNAs are known to have major functions in NSCLC development (5). In previous studies, NSCLC metastasis was suppressed by manipulating select miRNAs in preclinical experiments (6,7). Further, there is increasing evidence that miRNAs are major factors affecting metastasis, and such findings may lead to the development of new treatments for BM (8-10).

Proteomics is presently considered a major tool for the global assessment of protein expression, and has wide application in the field of cancer research. Quantitative protein expression profiling is an important part of proteomic analysis (11). Such profiling analyses have been used to screen metastasis-associated proteins in recent studies (12,13).

Rare studies used combined analysis of miRNA and proteome expression to explore the mechanism of lung adenocarcinoma (LAC) BM. In this study, we analyzed the pathogenesis of LAC—induced BM by detecting miRNA and proteome expression differences between primary LAC lesion and BM tissue specimens to identify the biomarkers of LAC-associated BM and develop potential therapeutic targets. We present the following article in accordance with the STREGA reporting checklist (available at https://atm.amegroups.com/article/view/10.21037/atm-22-5703/rc).

Highlight box

Key findings

- This study extended understandings of the regulatory network of miRNAs and proteins and provided novel insights into the pathogenic mechanisms of BM in LAC at the miRNA and protein levels.

What is known and what is new?

- Rare studies used combined analysis of miRNA and proteome expression to explore the mechanism of LAC.
- We combined analysis miRNAs and proteomic to explore the pathogenesis of brain metastasis of LAC.

What is the implication, and what should change now?

- These findings provide new insights into the mechanisms of LAC-associated BM and may extend understandings of the complex pathogenetic mechanisms underpinning BM, which could ultimately result in the design of new therapeutic strategies.

Methods

Samples

We conducted a retrospective study. The study was conducted in accordance with the Declaration of Helsinki (as revised in 2013). This study was approved by the Medical Ethics Committee of Peking University International Hospital [Approval No. 2020-060(BMR)] and informed consent forms were signed by all the patients. From September 2018 to October 2019, participants with histologically confirmed LAC treated at Peking University International Hospital were recruited. To be eligible for inclusion in this study, patients had to meet the following inclusion criteria: (I) have a diagnosis of LAC or LAC-associated BM by surgery; (II) have an Eastern Cooperative Oncology Group performance status (ECOG-PS) score between 0 and 2; (III) have normally functioning bone marrow, heart, liver, kidney, and other major organs; (IV) have a life expectancy >3 months; and (V) have complete circulating tumor deoxyribonucleic acid (DNA) assays for tissue specimens. Patients were excluded from the study if they met any of the following exclusion criteria: (I) had multiple primary carcinomas; (II) had a severe systemic disease; (III) had an active infection; and/or (IV) had an immune disease. The data collected included age, gender, and smoking history data.

The LAC participants were divided into the lung primary (LP) group (n=5, named L1, L2, L3, L4, and L5) and the BM group (n=5, named B1, B2, B3, B4, and B5). Tissues from the primary tumor sites in the LP group and from the BM tumor sites in the BM group were sampled. The tissues were fixed with 10% neutral buffered formalin within 5 minutes of excision, then fixed for 48 h, and after that embedded in paraffin. The samples were stored at 4 ℃ awaiting analysis. Next, the tissue blocks were sectioned at 5 μm. The unstained sections were used for the RNA extraction. After hematoxylin and eosin staining, tumor location was determined under a microscope, and sections of adjacent layers were taken.

© Annals of Translational Medicine. All rights reserved.

RNA extraction and sequencing

Total RNA was purified from formalin-fixed paraffin-embedded (FFPE) tumors with TRIzol reagent (Invitrogen, USA). RNA purity and integrity were assessed on an Agilent 2100 Bioanalyzer (Agilent, USA). Qualified RNA specimens (RNA integrity number ≥8 and 28S/18S ≥1) were used for the complementary DNA library generation. The Illumina HiSeq 2000 sequencing platform (Illumina, USA) was used for the RNA-sequencing.

LC-MS/MS

The liquid chromatography tandem mass spectrometry (LC-MS/MS) system included an Easy nLC1000 (Thermo Fisher, USA) coupled ultra-high resolution mass spectrometer Orbitrap Fusion Lumos (Thermo Fisher, USA) with a Thermo Fisher electrospray source. Each injection was first sent to a preset column (Acclaim PepMap C18, 100 μm × 2 cm; Thermo Fisher, USA) for adsorption at 3 L/min. Each sample was then sent to the analysis column (Acclaim PepMap C18, 75 μm × 15 cm; Thermo Fisher, USA) for separation.

The MS was carried out in the OT (Orbitrap)-OT mode. For a complete first-level scan, an AGC Target of 5E5 was set, with a scanning range of 350–1,550 m/z, a resolution of 120,000, and a maximum injection time of 50 ms. The second scan had a cycle time of 3.5 s and a collision energy of 32%; peptides with a charge between 2 and 7 were further fragmented. Maxquant 1.6.2.10 was used for the data analysis. Mass tolerance was 20 ppm with a false discovery rate (FDR) of 1%.

Data quality control

The raw reads obtained comprised low-quality reads, including those with missing insert tags, oversized inserts, poly(A) tags, and small tags. Data cleaning was thus performed on the raw reads from the Illumina sequencing platform to obtain the final clean reads, as follows: (I) reads in which more than 50% of bases had a Qphred ≤5 were discarded; (II) reads in which N (indeterminable base information) accounted for >10% were discarded; (III) reads with 5' primer contamination were discarded; (IV) reads lacking a 3' primer or insert tag were discarded; (V) the 3' primer sequences were trimmed; and (VI) reads with poly(A), poly(T), poly(G), or poly(C) tails were discarded.

Prediction of novel miRNAs

The small RNA (sRNA) reads underwent mapping to the genome with Bowtie to analyze their expression and genomic distributions. The above reads on the reference sequence were aligned with a specific sequence in the miRbase (https://www.mirbase.org/) to obtain sRNA details for a given sample match (e.g., the secondary structure of the matched miRNA, the miRNA sequence and length for each sample, occurrence number, and other information). Next, mirdeep2 was used to predict novel miRNAs (14).

Gene Ontology (GO) and Kyoto Encyclopedia of Genes and Genomes (KEGG) enrichment analyses of the target genes of the differentially expressed miRNAs and proteins

A GO enrichment analysis of the target genes for the differential miRNAs was performed with topGO in R, correcting for gene length bias. GO terms with corrected P values <0.05 were considered significantly enriched by the differential genes. For the KEGG pathway analysis (http://www.genome.jp/kegg/), clusterProfiler in R was used to retrieve the pathways significantly enriched by the differential genes.

Statistical analysis

SPSS v20.0 (IBM SPSS Statistics, USA) and R software v4.0.3 were used for the data analysis. The independent sample *t* test was used for comparisons between groups; a 1-way analysis of variance (ANOVA) was used for multiple comparisons. A P value <0.05 was considered statistically significant. To control for multiple testing, FDR estimation was carried out (15). To evaluate significance, a linear model was used for the continuous covariables, and an ANOVA was used for the categorical covariables.

Results

Data quality control

The age and gender of patients are described in *Table 1*, and no patients had a smoking history. RNA was extracted from the FFPE tumor specimens as described in method section. The results are shown in *Table 2*. The proportions of specimens with quality scores ≥20 (Q20) and ≥30 (Q30) were above 98% and 94%, respectively. A single base error rate of 0.001 was adopted.

© Annals of Translational Medicine. All rights reserved.

Table 1 Patient characteristics

Sample	Gender	Age (years)	Smoking history
BM1	Male	63	No
BM2	Male	75	No
BM3	Female	82	No
BM4	Female	52	No
BM5	Female	48	No
LP1	Female	70	No
LP2	Male	66	No
LP3	Female	60	No
LP4	Male	62	No
LP5	Female	57	No

BM, brain metastasis; LP, lung primary.

Table 2 Data quality control results

Sample	Raw reads	Bases	GC (%)	Q20	Q30	Avg. quality score
BM1	3839266	0.192 (GB)	53	98.63%	95.68%	35.83
BM2	3735819	0.187 (GB)	53	98.60%	95.61%	35.82
BM3	4123090	0.206 (GB)	53	98.58%	95.50%	35.8
BM4	3340001	0.167 (GB)	53	98.48%	95.38%	35.77
BM5	4210563	0.211 (GB)	54	98.16%	94.84%	35.66
LP1	3679273	0.184 (GB)	52	98.54%	95.32%	35.77
LP2	3834373	0.192 (GB)	52	98.64%	95.60%	35.82
LP3	5482979	0.274 (GB)	53	98.74%	95.82%	35.86
LP4	3604748	0.180 (GB)	52	98.73%	95.88%	35.87
LP5	7561029	0.378 (GB)	52	98.37%	95.49%	35.77

GC, guanine-cytosine; Q, quality score; BM, brain metastasis; LP, lung primary; GB, gigabase.

Differential miRNAs and proteins

A bioinformatics analysis was carried out to screen out miRNAs and proteins with differential expression between the LP and BM groups. Volcano plots were used to provide a visual representation of the differentially expressed miRNAs and proteins (*Figure 1*). In *Figure 1*, the x- and y-axes represent logarithmic fold changes (FCs) in miRNA or protein expression between the 2 groups and the negative logarithmic P values of miRNA or protein expression changes, respectively. A cut-off FC of 2 and a P value <0.05 were used as the criteria to confirm the significantly downregulated and upregulated miRNAs and proteins (FDR <0.05). In *Figure 1*, the red points represent the upregulated miRNAs or proteins in BM versus LP, while the green points represent the downregulated miRNAs or proteins.

The heatmaps (*Figures 2*,*3*) show significant changes in the miRNA and protein amounts between the LP and BM groups (FDR <0.05). The figures depict the bidirectional clustering of the differential miRNAs and proteins. The color depth indicates the expression level, with orange and purple representing high and low miRNA and protein amounts, respectively. The results suggested that 16 miRNAs, including miR-31-3p, miR-654-5p, miR-1185-1-3p, and miR-487a-5p, and 53 proteins, including VIM

© Annals of Translational Medicine. All rights reserved.

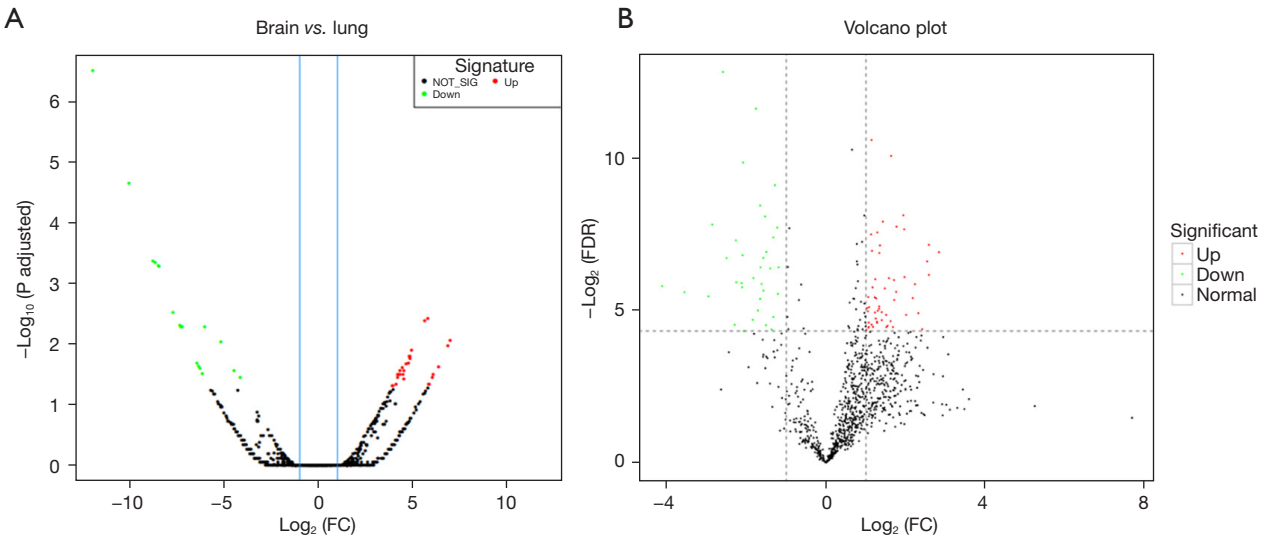

Figure 1 Volcano plots of differentially expressed miRNAs (A) and proteins (B). An absolute FC cut-off value of 2 and a P value <0.05 were used as the criteria to identify the significantly downregulated and upregulated miRNAs and proteins (FDR <0.05). The red points represent the upregulated miRNAs or proteins in BM *vs.* LP, and the green points represent the downregulated miRNAs or proteins in BM. FC, fold change; FDR, false discovery rate; miRNA, micro-ribonucleic acid; BM, brain metastasis; LP, lung primary.

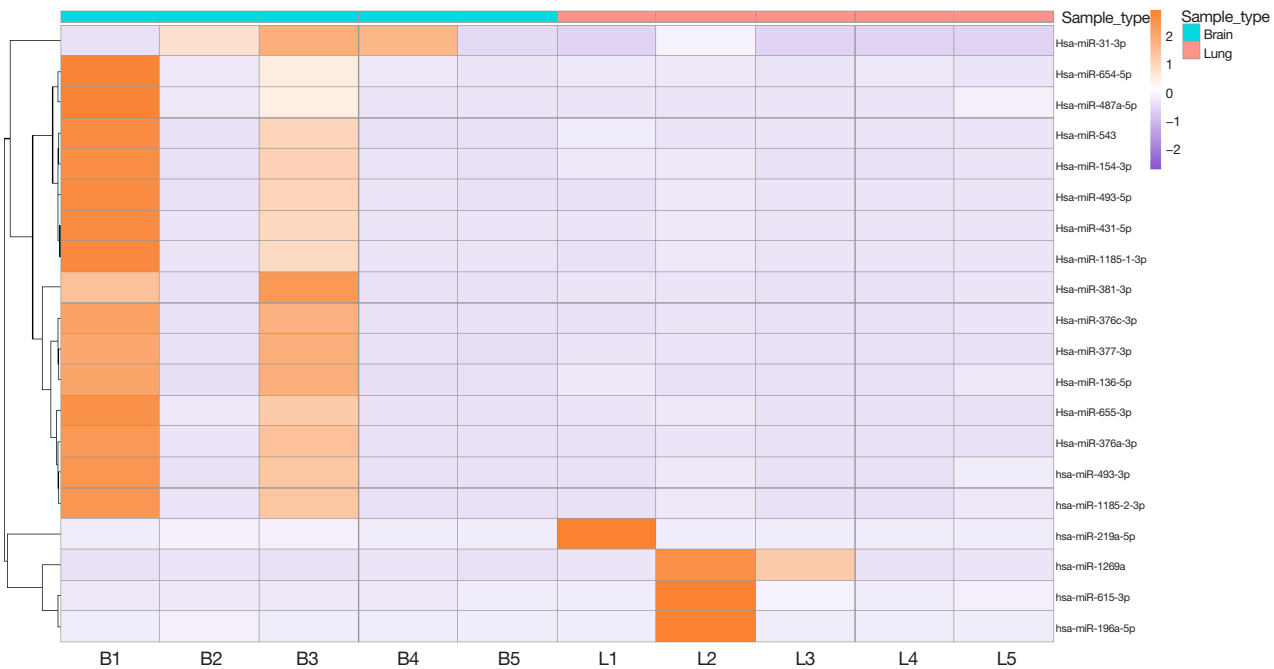

Figure 2 Heatmap of the differentially expressed miRNAs. Orange represents high levels and purple represents low levels of miRNA expression. miRNA, micro-ribonucleic acid.

© Annals of Translational Medicine. All rights reserved.

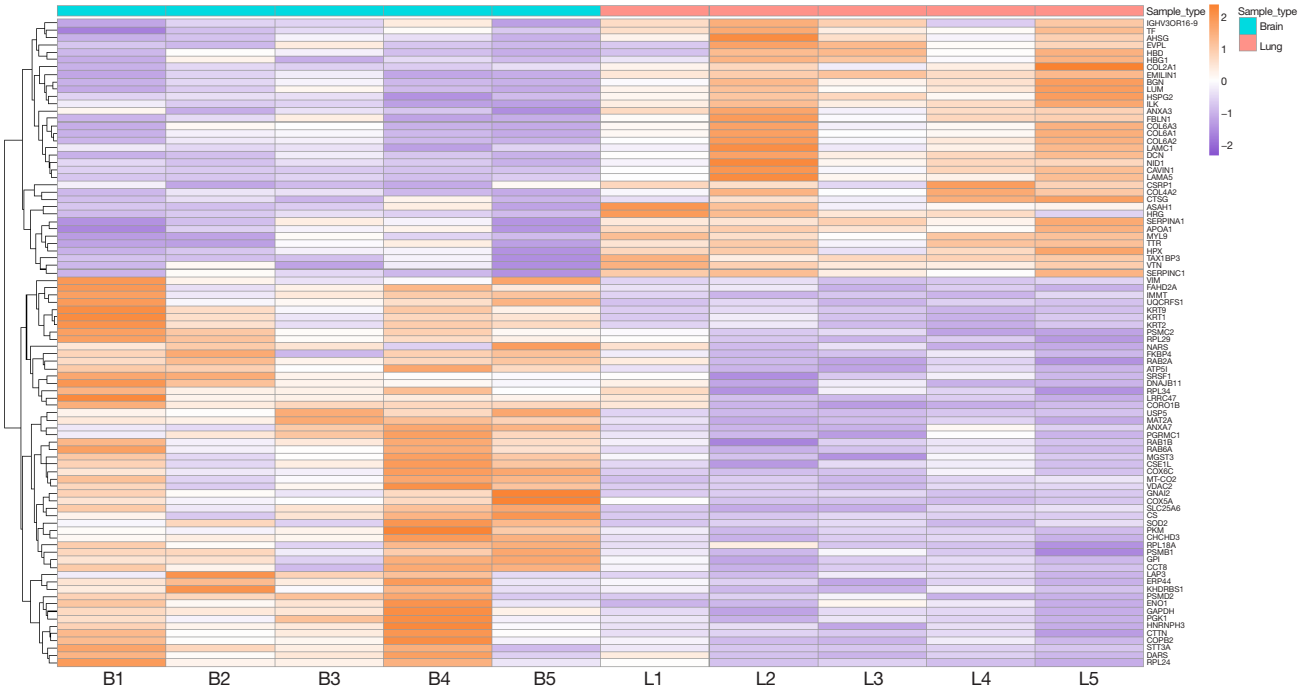

Figure 3 Heatmap of the differentially expressed proteins. Orange represents high levels and purple represents low levels of protein expression.

(Vimentin), RAB2A (RAB2A, member RAS oncogene family), RPLs (Ribosomal protein large subunit) and KRTs (Keratins), were significantly highly expressed in the BM patients, while miR-219a-5p, miR-1269a, miR-615-3p and miR-196a-5p (4 miRNAs) and Alpha 2-HS Glycoprotein (AHSG), Hemoglobin Subunit Delta (HBD), Serpin Family C Member 1 (SERPINC1), and Collagen Type VI Alpha 1 chains (COL6As) (a total of 35 proteins) were significantly lowly expressed, which may be related to the pathogenesis of BM.

An interaction network of differential miRNAs and proteins was obtained with Cytoscape and is depicted in *Figure 4*. In *Figure 4*, the nodes and edges represent the genes/proteins and the interactions among the genes/proteins, respectively; the black nodes represent the miRNAs, the green nodes represent the proteins. Red letters represent the miRNAs and proteins with high expression, while the blue letters represent the miRNAs and proteins with low expression; the lines represent the correlations and interactions among the genes and proteins.

Enrichment data

Based on expression differences, the differential miRNAs and proteins were categorized into upregulated and downregulated groups. The results of the GO enrichment analysis of the differentially expressed genes and proteins are depicted in *Figures 5*,*6*, respectively. The main enrichment data are included in the figures, and further information is summarized in the original result tables. In *Figure 5*, the ordinates and abscissas are the GO terms of the miRNAs and the numbers of enriched target genes, respectively. The differential miRNAs were enriched in a number of pathways, including binding, cell part, cell, organelle, intracellular organelle, and protein binding. In *Figure 6*, for the proteins, the abscissas are the GO terms; the numbers of target proteins and the percentages of target proteins are on the right and left, respectively. The differential proteins were enriched in a number of pathways, including the cellular process, cell, cell part, organelle, and binding. Both the enrichment analyses of the differentially expressed miRNAs and proteins revealed that cell, cell part, organelle, and binding signaling pathways have critical functions in the pathogenesis of LAC-associated BM.

KOBAS3.0 was used to analyze the enriched functional areas of the top 10 differential target genes of the miRNAs (*Figure 7*), which demonstrated that the differential miRNAs were mostly enriched in the extracellular vesicles, extracellular

© Annals of Translational Medicine. All rights reserved.

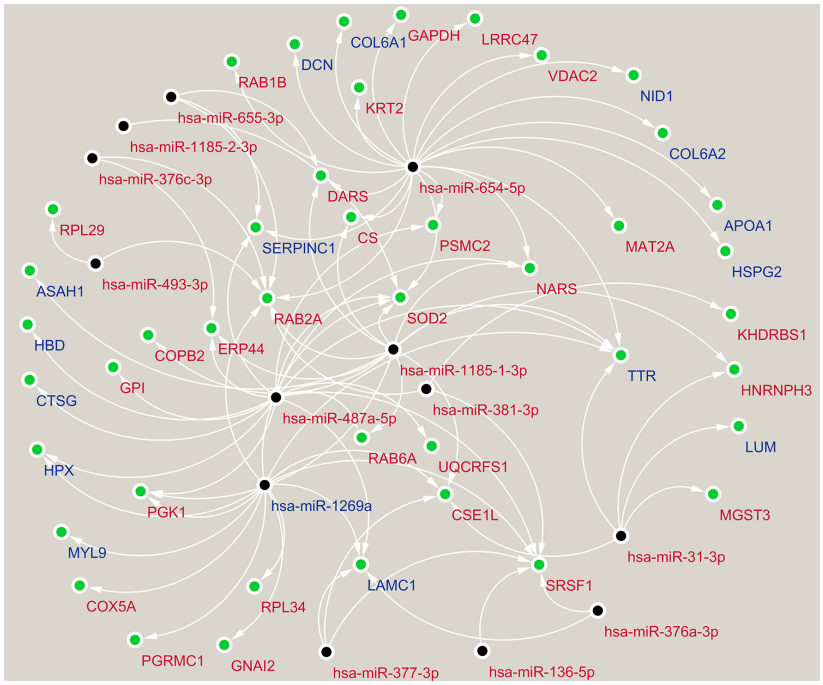

Figure 4 The interaction network of the differentially expressed miRNAs and proteins. The black nodes represent the miRNAs, the green nodes represent the proteins. Red letters represent the miRNAs and proteins with high expression, while the blue letters represent the miRNAs and proteins with low expression. The lines represent the correlations and interactions between the genes and proteins. miRNA, micro-ribonucleic acid.

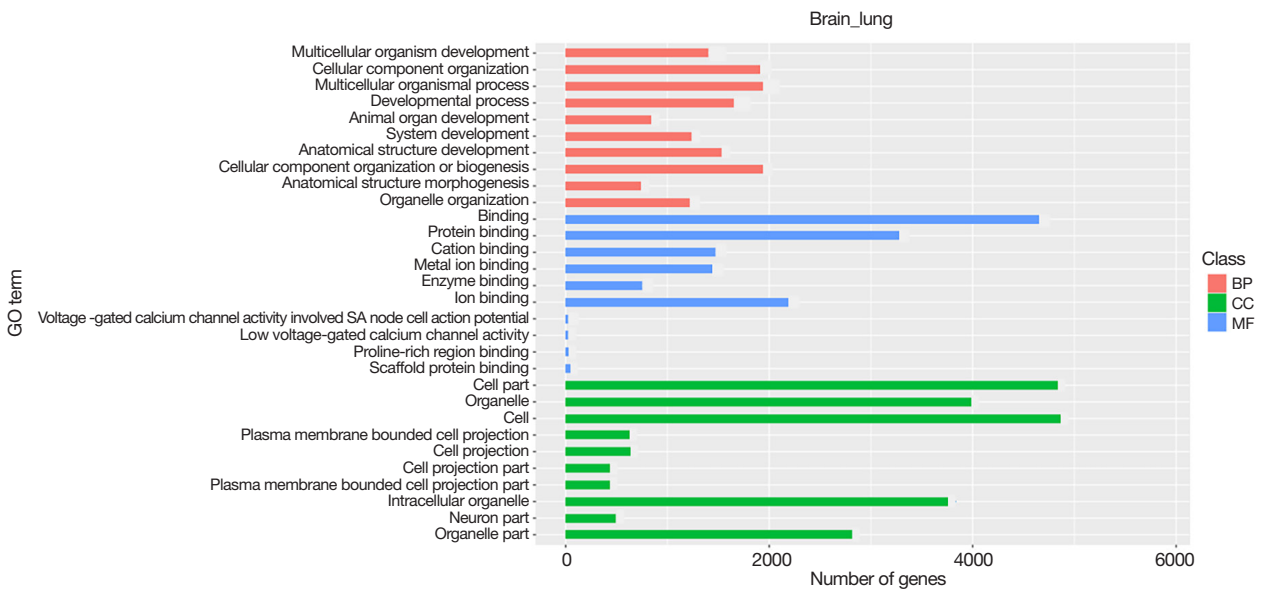

Figure 5 GO enrichment analysis of the differentially expressed miRNAs. The differentially expressed miRNAs were enriched in a number of signaling pathways, such as binding, cell part, cell, organelle, intracellular organelle, and protein binding. GO, Gene Ontology; BP, biological processes; CC, cellular components; MF, molecular functions; miRNA, micro-ribonucleic acid.

© Annals of Translational Medicine. All rights reserved.

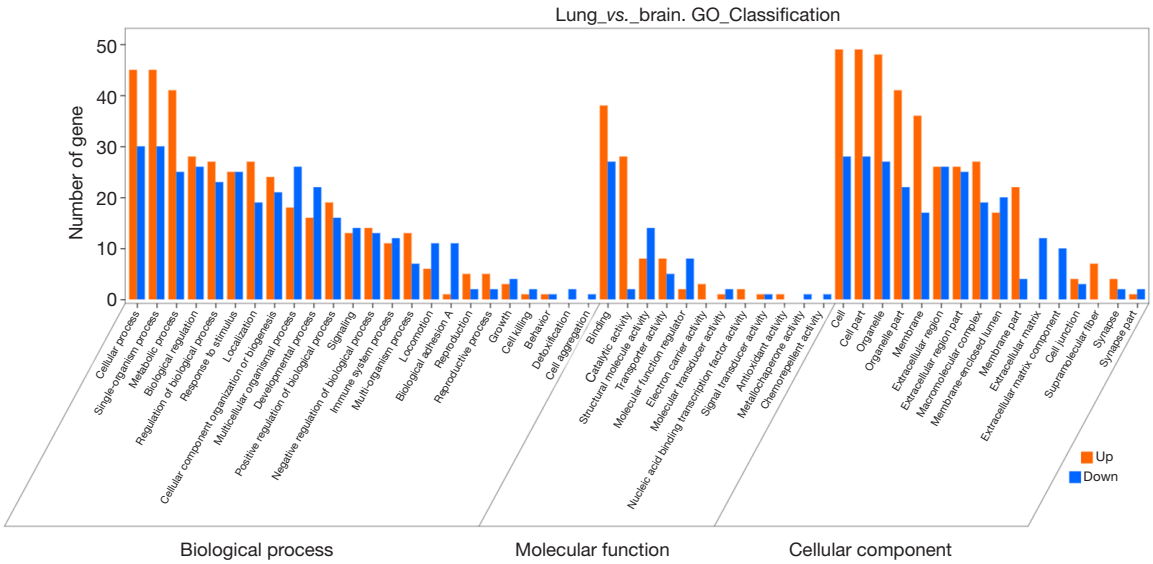

Figure 6 GO enrichment analysis of the differentially expressed proteins. The differentially expressed proteins were enriched in a number of signaling pathways, such as cellular process, cell, cell part, organelle, and binding. GO, Gene Ontology.

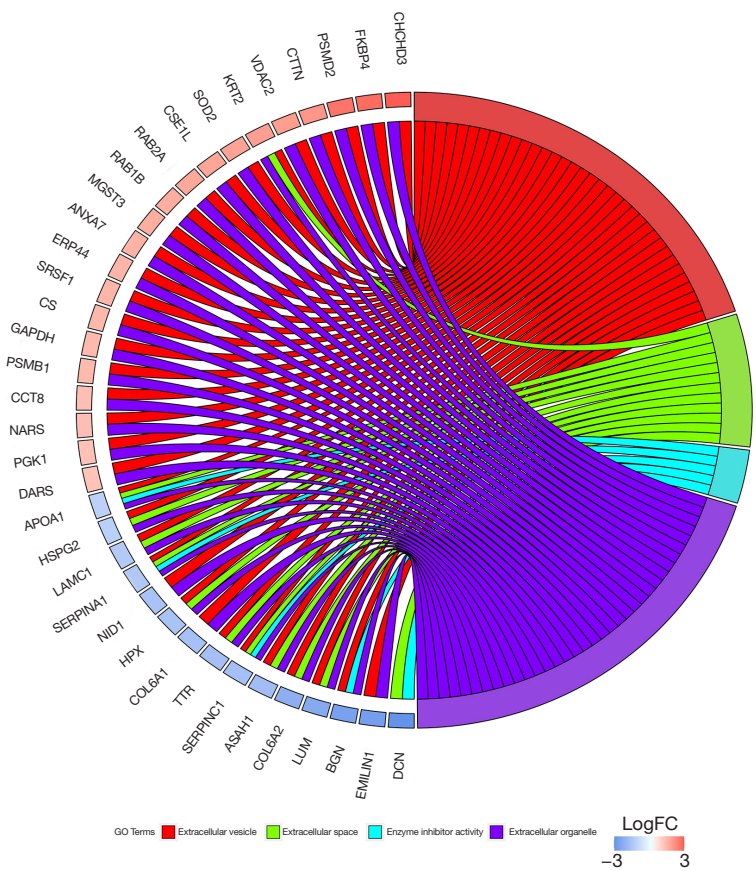

Figure 7 GO enrichment analysis of the top 10 significantly differentially expressed miRNA target genes. The differentially expressed miRNAs were mainly enriched in the extracellular vesicles, extracellular space, and functional areas of the extracellular organelles. GO, Gene Ontology; miRNA, micro-ribonucleic acid; FC, fold change.

© Annals of Translational Medicine. All rights reserved.

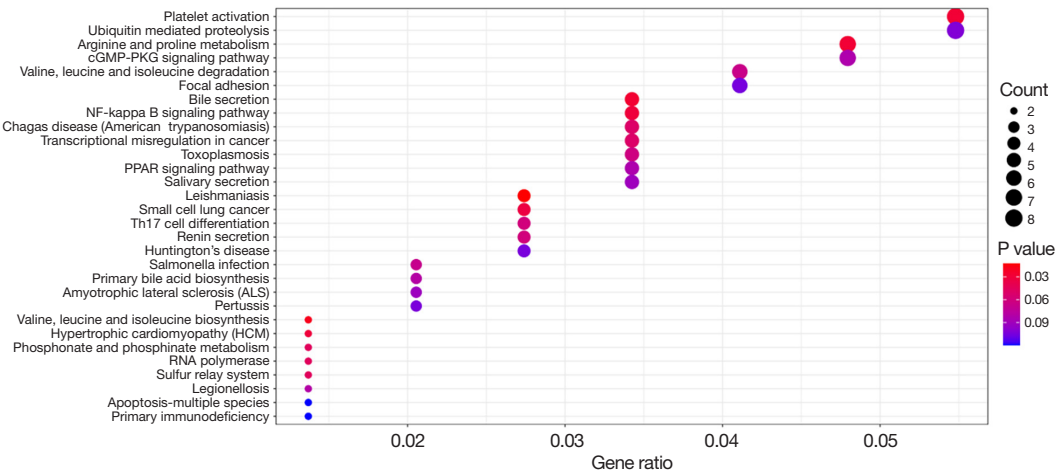

Figure 8 The bubble map of the KEGG enrichment analysis of the differentially expressed miRNAs. The top 30 pathways with the most significantly enriched miRNAs are shown in the item diagram. The ordinate describes the corresponding pathways, while the abscissa describes the enrichment factor; the bubble size is the number of different genes or proteins; the bubble color is the P value of enrichment significance. KEGG, Kyoto Encyclopedia of Genes and Genomes; miRNA, micro-ribonucleic acid.

space, and functional areas of the extracellular organelles.

The bubble map provides a graphical representation of the KEGG analysis results. The KEGG analysis was carried out to assess differentially expressed miRNAs and proteins, and the results are depicted in *Figures 8*,*9*, respectively. KEGG enrichment was measured by the gene ratio, P value, and the number of genes enriched in the given pathway. The gene ratio represents the ratio of the amount of differentially enriched genes to the total amount of differentially enriched genes in the given pathway. The higher the gene ratio, the greater the degree of enrichment. The p values ranged from 0 to 1; the closer the P value to 0, the more significant the enrichment. The top 30 pathways with the most significantly enriched miRNAs and the top 20 pathways of the proteins are shown in the item diagram. In *Figures 8*,*9*, the ordinates describe the respective pathways, while the abscissas show the enrichment factors; the bubble size and color represent the amounts of distinct genes/proteins and the P values for the enrichment significance, respectively. Both the enrichment analyses of the differential miRNAs and proteins showed that nuclear factor kappa B (NF-κB) signaling and primary immunodeficiency pathways are critical in the pathogenesis of LAC-associated BM.

Discussion

Messenger ribonucleic acids(mRNAs) in FFPE tumor specimens is degraded gradually, which will lead to unreliable transcriptome sequencing results, while proteins and miRNAs are relatively stable. Besides the protein is an encoding product which can represent the corresponding encoded mRNA. Therefore, we innovatively combined analysis miRNAs and proteomic to explore the pathogenesis of BM of LAC, which has not been conducted before. We found that compared to the LP group, 16 miRNAs and 53 proteins were significantly upregulated, while 4 miRNAs and 35 proteins were significantly downregulated in the BM group, which may be related to the pathogenesis of LAC-associated BM. We also found that tissue factor (TF) was lowly expressed in the BM group, which suggests that TF could inhibit the BM of LAC. These biomolecules may be potential diagnostic markers and drug targets, which will improve prediction of BM risk as well as the clinical treatment of LAD patients.

A previous study reported that metastasis preferentially occurred in organs expressing reduced TF amounts in the microcirculation, enabling tumor cell retention (16). Serpin Family A Member 1 was significantly differentially expressed between the BM and LP groups in the current study and another report (17). It has been reported that epithelial-to-mesenchymal transition–associated proteins and matrix metalloproteinases contribute to BM by modulating the blood-brain barrier (18). In addition, the high expression of inner membrane mitochondrial protein is closely associated with advanced disease stage and poor patient prognosis in LAC (19). Further, asparagine-tRNA

© Annals of Translational Medicine. All rights reserved.

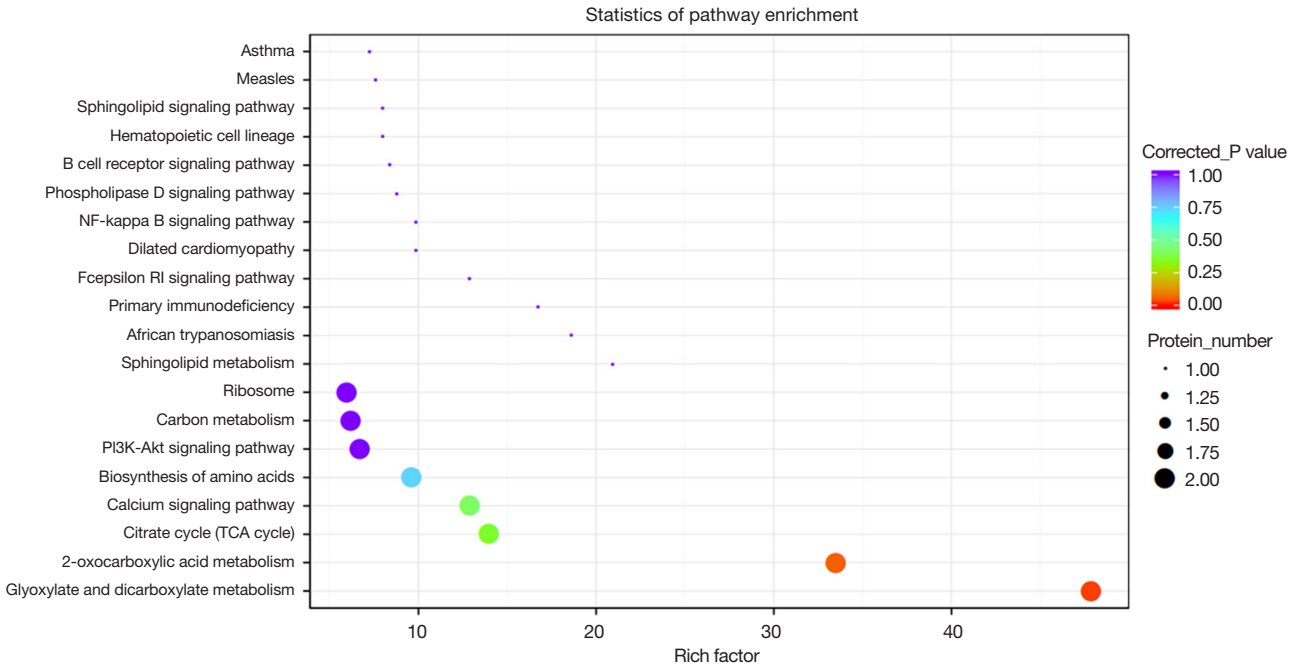

Figure 9 The bubble map of the KEGG enrichment analysis of the differentially expressed proteins. The top 20 pathways of the proteins are shown in the item diagram. The ordinate describes the corresponding pathways, while the abscissa describes the enrichment factor; the bubble size is the number of different genes or proteins; the bubble color is the P value of enrichment significance. KEGG, Kyoto Encyclopedia of Genes and Genomes.

ligase, cytoplasmic (NARS) levels have been found to be positively correlated with LAC lymph node metastasis (20). The above findings were consistent with this study. We also found that proteins, including KRTs, COL6As, RAB2A and AHSG, were associated with the pathogenesis of LAC-associated BM. However, the current trial had a small sample size, and more samples are needed for further confirmation.

MiR-31-3p is involved in the pathogenetic mechanisms of various malignancies, such as colorectal cancer, and lymph node metastasis and poor patient prognosis in LAC (21). As stated above, miR-31-3p was significantly increased in the BM group, which suggests that it may promote the occurrence and development of BM in LAC cases. MiR-493-5p is associated with the pathogeneses of various malignant tumors, such as liver cancer, colorectal cancer, and osteosarcoma, and patient prognosis in NSCLC. It can affect the malignant behavior of NSCLC cells by controlling integrin β1 expression (22). We found that miR-493-5p also promoted LAC-associated BM. These findings indicate that miRNAs could be used as biomarkers of the occurrence, progression, and prognosis, and potential therapeutic targets in lung cancer-associated BMs. In line with previous studies (21,22), this study also found these miRNAs had differential expression levels between the 2 groups, which suggests that these miRNAs are correlated with the pathogenesis of BM in LAC. In addition, we found differential expression for miR-487a-5p, miR-654-5p, miR-1185-1-3p, miR-376c-3p, and miR-196a-5p between the BM and LP groups for the first time, which may also contribute to the BM of LAC. Previous evidence indicates miR-654-5p promotes the progression of colon cancer (23), breast cancer (24), and oral squamous cell carcinoma (25), and induces ovarian cancer cell resistance to paclitaxel (26). The current research revealed that miR-654-3p may promote the progression of LAC-associated BM. MiR-1185-1-3p could be used for the early diagnosis in bladder cancer (27). We first reported the association of miR-1185-1-3p with BM in LAC, and no previous studies have focused on the associations of the above miRNAs with lung cancer or BM.

The enrichment analysis of differential miRNAs and differential proteins was conducted respectively, the pathway that both miRNAs and proteins were enriched is considered to be closely related to the pathogenesis of LAC BM. We found that the pathogenesis of BM in LAC involved NF-κB signaling, which corroborates previously reported data (28). Research has shown that primary

© Annals of Translational Medicine. All rights reserved.

immunodeficiency signaling also controls the occurrence and development of BM in LAC, which represents a novel mechanism. NF-κB signaling constitutes a major pathway in the development and metastases of various inflammatory and malignant tumors (e.g., breast and lung cancers) (28). In addition, previous studies have revealed multiple mechanisms underpinning the occurrence and progression of LAC-associated BM. The highly open calcium-activated potassium channels in lung cancer-associated BM and the respective microvascular endothelial cells could be used as targets for blood-brain tumor barrier and permeability regulation (29). Vascular endothelial growth factor C plays a role in the pathogenesis of lung cancer-induced BM by enhancing tumor cell affinity to particular organs and promoting tumor cell movement to lymphatic vessels (30,31). The interaction between neurotransmitter receptors and neurons could induce lung cancer metastasis to the brain (31). The abnormal expression of tumor suppressor genes, matrix metalloproteinases, carcinoembryonic antigen, and other associated proteins may also contribute to LAC-related BM.

This research had some limitations. First, in the present study, we did not obtain samples from primary and metastatic lesions from the same patient, which could have been used to exclude the interference of expression differences caused by histological differences in brain and lung tissues. Relevant samples will be collected in the future for further studies. Additionally, multiple studies have examined the expression levels of cerebrospinal fluid miRNAs and proteins in central nervous system-associated malignant tumors, and their diagnostic and application values. For example, it was found that differentially expressed miRNAs in the cerebrospinal fluid could distinguish glioblastoma from metastatic brain malignancies and may be used to monitor changes in disease condition and responses to treatment (32). Due to the difficulty in obtaining BM tissue specimens, subsequent attempts should be made to explore the feasibility of using cerebrospinal fluid specimens from BM and non-BM cases to detect differentially expressed non-coding RNAs and proteins.

Finally, a due to the limitations of the small sample size and cohort selection in the present study, a larger cohort is required to examine and validate the current data.

Conclusions

In conclusion, RNA-sequencing and proteomics revealed many players involved in LAC-associated BM. These findings provide new insights into the mechanisms of LAC-associated BM and may extend understandings of the complex pathogenetic mechanisms underpinning BM, which could ultimately result in the design of new therapeutic strategies.

Acknowledgments

Funding: This work was supported by the Beijing Xisike Oncology Research Foundation (Nos. Y-HS2019/2-056, Y-HR2018-315).

Footnote

Reporting Checklist: The authors have completed the STREGA reporting checklist. Available at https://atm.amegroups.com/article/view/10.21037/atm-22-5703/rc

Data Sharing Statement: Available at https://atm.amegroups.com/article/view/10.21037/atm-22-5703/dss

Conflicts of Interest: All authors have completed the ICMJE uniform disclosure form (available at https://atm.amegroups.com/article/view/10.21037/atm-22-5703/coif). The authors have no conflicts of interest to declare.

Ethical Statement: The authors are accountable for all aspects of the work in ensuring that questions related to the accuracy or integrity of any part of the work are appropriately investigated and resolved. The study was conducted in accordance with the Declaration of Helsinki (as revised in 2013). The study was approved by the Medical Ethics Committee of Peking University International Hospital [Approval No. 2020-060(BMR)] and informed consent was taken from all the patients.

Open Access Statement: This is an Open Access article distributed in accordance with the Creative Commons Attribution-NonCommercial-NoDerivs 4.0 International License (CC BY-NC-ND 4.0), which permits the non-commercial replication and distribution of the article with the strict proviso that no changes or edits are made and the original work is properly cited (including links to both the formal publication through the relevant DOI and the license). See: https://creativecommons.org/licenses/by-nc-nd/4.0/.

References

1. Zimmermann S, Dziadziuszko R, Peters S. Indications and limitations of chemotherapy and targeted agents in non-

© Annals of Translational Medicine. All rights reserved.

small cell lung cancer brain metastases. Cancer Treat Rev 2014;40:716-22.
2. Sperduto PW, Kased N, Roberge D, et al. Summary report on the graded prognostic assessment: an accurate and facile diagnosis-specific tool to estimate survival for patients with brain metastases. J Clin Oncol 2012;30:419-25.
3. Lu TX, Rothenberg ME. MicroRNA. J Allergy Clin Immunol 2018;141:1202-7.
4. Iorio MV, Croce CM. MicroRNA dysregulation in cancer: diagnostics, monitoring and therapeutics. A comprehensive review. EMBO Mol Med 2012;4:143-59.
5. Arora S, Ranade AR, Tran NL, et al. MicroRNA-328 is associated with (non-small) cell lung cancer (NSCLC) brain metastasis and mediates NSCLC migration. Int J Cancer 2011;129:2621-31.
6. Wu X, Liu T, Fang O, et al. MicroRNA-708-5p acts as a therapeutic agent against metastatic lung cancer. Oncotarget 2016;7:2417-32.
7. Wang X, Chen X, Meng Q, et al. MiR-181b regulates cisplatin chemosensitivity and metastasis by targeting TGFβR1/Smad signaling pathway in NSCLC. Sci Rep 2015;5:17618.
8. Wei C, Zhang R, Cai Q, et al. MicroRNA-330-3p promotes brain metastasis and epithelial-mesenchymal transition via GRIA3 in non-small cell lung cancer. Aging (Albany NY) 2019;11:6734-61.
9. Alsidawi S, Malek E, Driscoll JJ. MicroRNAs in brain metastases: potential role as diagnostics and therapeutics. Int J Mol Sci 2014;15:10508-26.
10. Sun G, Ding X, Bi N, et al. Molecular predictors of brain metastasis-related microRNAs in lung adenocarcinoma. PLoS Genet 2019;15:e1007888.
11. Liu YF, Chen YH, Li MY, et al. Quantitative proteomic analysis identifying three annexins as lymph node metastasis-related proteins in lung adenocarcinoma. Med Oncol 2012;29:174-84.
12. Kalita-de Croft P, Straube J, Lim M, et al. Proteomic Analysis of the Breast Cancer Brain Metastasis Microenvironment. Int J Mol Sci 2019;20:2524.
13. Huang H, Liu R, Huang Y, et al. Acetylation-mediated degradation of HSD17B4 regulates the progression of prostate cancer. Aging (Albany NY) 2020;12:14699-717.
14. Friedländer MR, Mackowiak SD, Li N, et al. miRDeep2 accurately identifies known and hundreds of novel microRNA genes in seven animal clades. Nucleic Acids Res 2012;40:37-52.
15. Liang J, Tong P, Zhao W, et al. The REST gene signature predicts drug sensitivity in neuroblastoma cell lines and is significantly associated with neuroblastoma tumor stage. Int J Mol Sci 2014;15:11220-33.
16. Nevo N, Ghanem S, Crispel Y, et al. Heparanase Level in the Microcirculation as a Possible Modulator of the Metastatic Process. Am J Pathol 2019;189:1654-63.
17. Zhang Z, Cui F, Zhou M, et al. Single-cell RNA Sequencing Analysis Identifies Key Genes in Brain Metastasis from Lung Adenocarcinoma. Curr Gene Ther 2021;21:338-48.
18. Feng X, Xu ES. Alectinib and lorlatinib function by modulating EMT-related proteins and MMPs in NSCLC metastasis. Bosn J Basic Med Sci 2021;21:331-8.
19. Hiyoshi Y, Sato Y, Ichinoe M, et al. Prognostic significance of IMMT expression in surgically-resected lung adenocarcinoma. Thorac Cancer 2019;10:2142-51.
20. Hsu CH, Hsu CW, Hsueh C, et al. Identification and Characterization of Potential Biomarkers by Quantitative Tissue Proteomics of Primary Lung Adenocarcinoma. Mol Cell Proteomics 2016;15:2396-410.
21. Wang Y, Shang S, Yu K, et al. miR-224, miR-147b and miR-31 associated with lymph node metastasis and prognosis for lung adenocarcinoma by regulating PRPF4B, WDR82 or NR3C2. PeerJ 2020;8:e9704.
22. Zhang C, Wu S, Song R, et al. Long noncoding RNA NR2F1-AS1 promotes the malignancy of non-small cell lung cancer via sponging microRNA-493-5p and thereby increasing ITGB1 expression. Aging (Albany NY) 2020;13:7660-75.
23. Huang F, Wu X, Wei M, et al. miR-654-5p Targets HAX-1 to Regulate the Malignancy Behaviors of Colorectal Cancer Cells. Biomed Res Int 2020;2020:4914707.
24. Shen P, Yu Y, Yan Y, et al. LncRNA CASC15 regulates breast cancer cell stemness via the miR-654-5p/MEF2D axis. J Biochem Mol Toxicol 2022;36:e23023.
25. Lu M, Wang C, Chen W, et al. miR-654-5p Targets GRAP to Promote Proliferation, Metastasis, and Chemoresistance of Oral Squamous Cell Carcinoma Through Ras/MAPK Signaling. DNA Cell Biol 2018;37:381-8.
26. Li ZY, Wang XL, Dang Y, et al. Long non-coding RNA UCA1 promotes the progression of paclitaxel resistance in ovarian cancer by regulating the miR-654-5p/SIK2 axis. Eur Rev Med Pharmacol Sci 2020;24:591-603.
27. Usuba W, Urabe F, Yamamoto Y, et al. Circulating miRNA panels for specific and early detection in bladder cancer. Cancer Sci 2019;110:408-19.
28. Chen Q, Boire A, Jin X, et al. Carcinoma-astrocyte gap junctions promote brain metastasis by cGAMP transfer. Nature 2016;533:493-8.

© Annals of Translational Medicine. All rights reserved.

29. Ningaraj NS, Rao M, Hashizume K, et al. Regulation of blood-brain tumor barrier permeability by calcium-activated potassium channels. J Pharmacol Exp Ther 2002;301:838-51.
30. Chen G, Liu XY, Wang Z, et al. Vascular endothelial growth factor C: the predicator of early recurrence in patients with N2 non-small-cell lung cancer. Eur J Cardiothorac Surg 2010;37:546-51.
31. Song P, Sekhon HS, Fu XW, et al. Activated cholinergic signaling provides a target in squamous cell lung carcinoma. Cancer Res 2008;68:4693-700.
32. Teplyuk NM, Mollenhauer B, Gabriely G, et al. MicroRNAs in cerebrospinal fluid identify glioblastoma and metastatic brain cancers and reflect disease activity. Neuro Oncol 2012;14:689-700.

(English Language Editor: L. Huleatt)

Cite this article as: Zhang L, Liang J, Han Z, Wang L, Liang J, Zhang S. Micro-ribonucleic acids (miRNAs) and a proteomic profile in lung adenocarcinoma cases with brain metastasis. Ann Transl Med 2022;10(24):1389. doi: 10.21037/atm-22-5703

© Annals of Translational Medicine. All rights reserved.